SACRAMENTO WASH 005 AND MET 00428: IMPACT GENERATED SULFIDE-RICH FE,NI MELTS FROM THE H-CHONDRITE PARENT BODY.
D. L. Schrader[1], H. C. Connolly, Jr.[1,2,3], and D. S. Lauretta[1]. [1]University of Arizona, Lunar and Planetary Laboratory (LPL), Tucson, AZ 85721, USA, schrader@lpl.arizona.edu, [2]Dept. Physical Sciences, Kingsborough College of the City University of New York, 2001 Oriental Blvd., Brooklyn N.Y. 100235, [3]Dept. Earth and Planetary Sciences, AMNH Central Park West, New York, N.Y. 110024.

Introduction: The H-chondrite parent body has undergone extensive impact cratering resulting in 25% of its members being breccias [1]. One impact has resulted in the metallic-melt breccia, Portales Valley (PV); whose Fe,Ni veins resemble the morphology of iron meteorites [2]. Ungrouped iron meteorites either represent single samples from individual parent bodies, or show unique alteration histories from parent bodies of recognized groups [3]. We report the results of our investigation to (1) characterize the S-rich, ungrouped iron meteorites Sacramento Wash 005 (SW), MET 00428 (MET), and HOW 88403 (HOW); (2) compare them to known meteorite groups; and (3) constrain the processes which formed them.

Analytical Procedure: We examined one polished thick section from SW, MET, and HOW. Quantitative analyses were performed on the Cameca SX-50 EMP at LPL using an accelerating voltage of 15 kv and a beam current of 40 nA for metal analyses, and 15 kv and 20 nA for silicates. The concentrations of S, Cr, Mn, Ti, Fe, Ni, Co, Cu, Na, K, Si, Mg, Al, P, and Ca were analyzed. Bulk and trace element abundances were obtained on the ELEMENT2 HR-ICP-MS at LPL; with two samples of SW (Table 1, Fig. 1).

Results: *Sacramento Wash 005* contains Fe,Ni metal, troilite, metallic copper, chromite, Ca-phosphate, iron-oxide, and a copper-iron-sulfide. The silicate inclusion within the sample contains Fe,Ni metal, troilite, olivine, pyroxene, plagioclase, and Ca-phosphate. The silicate inclusion has an irregular shape and contains predominately porphyritic olivine-pyroxene (POP) chondrules with minor amounts of cryptocrystalline (C) and radiating pyroxene (RP) chondrules (Fig. 2). All chondrules have sharp boundaries and range in apparent diameter from 0.13-0.35mm. A sharply defined POP chondrule borders the Fe,Ni metal host. The inclusion is a fragment of an H4 chondrite.

Troilite comprises ~26% of the cross-sectional surface area of the metallic portion. It is present as elongated inclusions in the Fe,Ni metal with apparent long axes ranging from 0.1-2.0 mm (Fig. 2). No Widmanstätten pattern is present. While kamacite is dominant, taenite is present as exsolution lamellae with widths ranging from 5-100 µm. The silicate compositions are; $Fa_{16.7-20.6}$ (average = $Fa_{17.4\pm0.8}$), $Fs_{6.2-19.9}$ (average = $Fs_{15.2\pm1.9}$) and $Wo_{0.38-46.0}$ (average = $Wo_{3.0\pm8.0}$).

MET 00428 contains kamacite, taenite, metallic copper, troilite, calcium-phosphate, and pyroxene. A weak Widmanstätten pattern is present, with kamacite bands ranging from 100-200 µm [4]. Kamacite is dominant, with taenite present as exsolution lamellae with widths ranging from 5-200 µm. The troilite is present as elongated blebs ranging from 0.1-1.5 mm in apparent length within the Fe,Ni metal. Swathing kamacite surrounds troilite blebs. The troilite inclusions comprise ~12% of the cross-sectional surface area of the sample. Three small (~20-40 µm) rounded, homogeneous silicate inclusions of pyroxene are associated with troilite inclusions, one of which borders kamacite. The small silicate inclusions are equilibrated pyroxene; $Fs_{16.8-17.8}$ (average = $Fs_{17.3\pm0.3}$) and $Wo_{1.1-3.1}$ (average = $Wo_{2.3\pm0.8}$).

HOW 88403 contains kamacite, taenite, troilite, schreibersite, chromite, and silica. The meteorite exhibits an ataxite structure [5]. Kamacite is dominant, with taenite exsolution lamellae ranging from 1-10 µm. Troilite is present as elongated blebs within the Fe,Ni metal, ranging from 0.1-2.25 mm. The troilite inclusions comprise ~31% of the cross-sectional surface area of the sample. Schreibersite almost completely surrounds the troilite blebs. An inclusion comprised of silica is surrounded by chromite and troilite.

Table 1. ICP-MS Bulk Analyses

		Sacramento Wash 005 1	Sacramento Wash 005 2	MET 00428	HOW 88403
Fe	Wt%	88 (1)	90 (1)	89 (1)	87 (2)
Ni	Wt%	7.6 (.1)	6.3 (.1)	6.9 (.2)	7.3 (.1)
Co	Wt%	0.36 (.01)	0.39 (.01)	0.47 (.01)	0.41 (.01)
S	Wt%	3.9 (.1)	3.8 (.1)	2.6 (.1)	4.3 (.1)
As	ppm	7.4 (.2)	9.2 (.3)	9.1 (.3)	7.3 (.4)
Ga	ppm	20.6 (.7)	17.3 (.6)	14.8 (.4)	19.4 (.6)
Ge	ppm	39 (2)	60 (2)	50 (2)	46 (1)
Ir	ppm	3.0 (.1)	3.1 (.2)	6.1 (.1)	4.4 (.1)

Discussion: Comparison to known meteorite groups suggests that SW and MET are related to the H-chondrites. HOW shows similarities, but its relationship is uncertain.

Compared to the iron meteorite chemical groups, SW, MET, and HOW are chemically closest to the low

Ni end of the IIIAB group (Fig. 1). Yet, they do not have a metal morphology similar to the IIIABs and are not chemically similar to the S-rich IIIABs, Bear Creek and Bella Roca [6]. Ni vs. Ir data from the largest metal grains in H-chondrites from [7] plot near SW, MET, and HOW, suggesting a relationship to the H-chondrites. SW and MET have silicate compositions within the range for H-chondrites, and SW's is morphologically identical to the H4-chondrites.

Based on kamacite lamellae widths within MET, and assuming kamacite widths are directly proportional to taenite widths for SW and HOW, apparent cooling rates can be inferred to be rapid (perhaps hundreds of °C/Myr [8, 9]); HOW cooled fastest, followed by SW and MET. The sulfide abundance within SW, MET, and HOW correlate with our inferred cooling rates: the quicker these samples cooled, more sulfide was trapped (Table 1). Comparing our findings to PV metal veins, it clearly cooled more slowly than our samples and thus retained no S [2].

To obtain the metal-sulfide morphology observed in SW, MET, and HOW, the peak melting temperature must have been above the Fe-FeS eutectic of 988 °C. Also, the melt material must have been buried quickly after impact or never been exposed on the surface, as S would have evaporated if the melt was left to cool on the surface. As chondrule boundaries are well defined in SW, the silicate was not exposed to temperatures above 950 °C [10] at length. Therefore SW's silicate inclusion appears to have been introduced into the metal-sulfide melt as it was cooling (i.e. regolith filling the crater, burying the melt), or the sample cooled below 950 °C so rapidly the silicate did not have time to melt. The silicate inclusions in MET suggest they were once melted, placing a higher upper boundary on formation temperature (above 950 °C).

PV metal data from [2] does not plot near SW, MET, or HOW in Ni vs. Ga or Ni vs. Ge plots; this could be due to the much slower cooling rate of PV relative to SW, MET, and HOW, or a sampling issue due to the sulfides. Alternatively, PV may have formed at depth [2], with the location of formation influencing trace-element composition.

Conclusion: The most likely formation process for SW and MET is impact induced melting on the H-chondrite parent body, not from core-mantle differentiation of a large asteroid. The differences between SW and MET could be the result of local compositional variations within the same impact crater, depth below the impact crater, or the result of separate impact craters (i.e. different local chemistry, T, P, cooling rates, etc.) on the H-parent body. However, HOW may have formed by impact, but its relationship to known meteorite groups is unclear. The samples cooled rapidly near the surface and trapped sulfides; they were either quickly buried or never exposed.

References: [1] Keil K. (1982) in *Workshop on Lunar Breccias and Soils and their Meteoritic Analogs*, 65–83. [2] Ruzicka A. et al. (2005) *Meteoritics & Planet. Sci.*, *40*, 261-295. [3] Weisberg M. K. et al. (2006) in *MESS II*, 19–52. [4] Russell S. S. et al (2002) *Meteoritics & Planet. Sci.*, *37*, A157-A184. [5] Grossman J. N. (1994) *Meteoritics*, *29*, 100-143. [6] Wasson J. T. (1999) *GCA*, *63*, 2875–2889. [7] Rambaldi E. F. et al. (1977) *Earth Planet. Sci. Lett.*, *36*, 347-358. [8] Short J. M. and Goldstein J. I. (1967) *Science*, *156*, 59-61. [9] Saikumar V. and Goldstein J. I. (1988) *GCA*, *52*, 715-726. [10] Brearley A. J. and Jones R. H. (1998) in *Planetary Materials*, 3-398.

Acknowledgements: The authors thank K. Domanik, J. Goreva, D. Hill, T. McCoy, L. Welzenbach, P. Meyers, J. Smaller, and MWG. This research was funded in part by NASA grant NNX07AF96G (DSL, PI) and NNG05GF39G (HCCJr, PI).

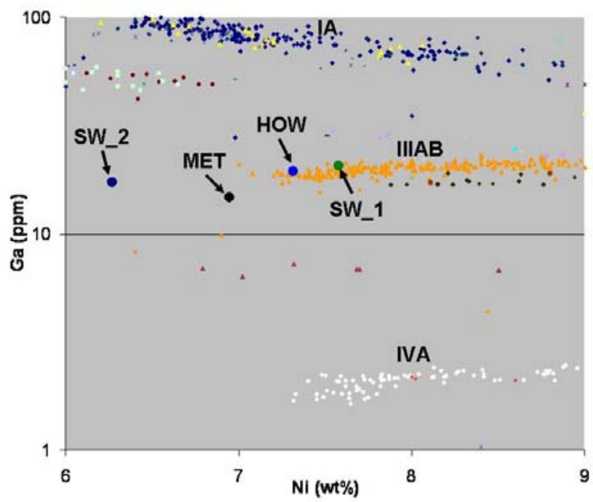

Figure 1. Ni vs Ga: Iron data from MetBase 6.0 plotted with the samples of this study.

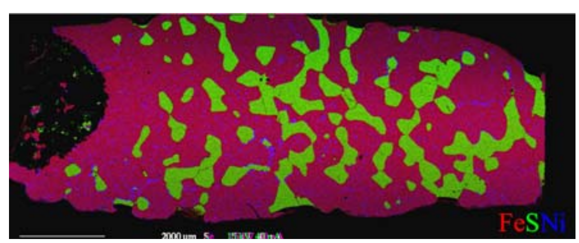

Figure 2. Sacramento Wash 005: RGB X-Ray Map showing sulfides, Fe,Ni metal host, and silicate inclusion (far left).